

Direct displacement-based design for RC structures – Procedure, advantages and shortcomings

Método de dimensionamento com base em deslocamentos para estruturas em betão armado – Procedimento, vantagens e limitações

Beatriz Massena
Rita Bento
Hervé Degée
Paulo Candeias

Abstract

In the early nineties, the Performance-Based Seismic Engineering (PBSE) principles have been introduced in the seismic design of structures. Several authors have identified the limitations of traditional force-based design (FBD) procedures widespread in most of the design codes to accomplish the PBSE requirements. Therefore, various contributions were made towards the development of displacement-based seismic design methodologies, in particular the one proposed by Priestley, known as "Direct Displacement-Based Design" (DDBD). The purpose of this work is to investigate the DDBD approach in its entirety. In particular, the emphasis is set herein on the definition of the equivalent viscous damping and on the concrete impact of choosing one or another expression. Then, the efficiency of applying DDBD to reinforced concrete (RC) plane frames and dual frame-wall structures is assessed and the consequences of using the linear response spectrum suggested in the Eurocode 8 as input data is investigated.

Resumo

Os métodos de avaliação sísmica com base no desempenho, particularmente os baseados em deslocamentos, têm sido introduzidos no dimensionamento sísmico de estruturas. Diversos autores identificaram limitações inerentes aos métodos de dimensionamento com base em forças (FBD), tradicionalmente implementados nos regulamentos sísmicos, de forma a cumprirem os níveis de desempenho em concordância com aquela nova filosofia de dimensionamento. Os métodos de dimensionamento com base em deslocamentos têm ganho popularidade e várias propostas surgiram, destacando-se o método "Dimensionamento Direto com Base em Deslocamentos" (DDBD), proposto por Priestley.

O objetivo deste trabalho é investigar o método DDBD, na sua globalidade, sendo dada ênfase à definição do amortecimento viscoso equivalente. Posteriormente é avaliada a eficiência do método DDBD no dimensionamento de estruturas planas de betão armado: pórticos e mista pórtico-parede, e comparado com o método FBD, proposto no Eurocódigo 8, recorrendo a análises dinâmicas lineares por espectro de resposta.

Keywords: Direct displacement-based design / Equivalent viscous damping / Reinforced concrete buildings

Palavras-chave: Dimensionamento baseado em deslocamentos / Amortecimento viscoso equivalente / Edifícios de betão armado

Beatriz Massena

PhD in Civil Engineering/Civil Engineering
HTB Consult, Lda.
Lisbon, Portugal
bmassena@htb.pt

Rita Bento

Associate Professor with Habilitation
Instituto Superior Técnico
Lisbon, Portugal
rita.bento@tecnico.ulisboa.pt

Hervé Degée

Associate Professor
Hasselt University
Hasselt, Belgium
Herve.degee@uhasselt.be

Paulo Candeias

Assistant Researcher
LNEC
Lisbon, Portugal
pcandeias@lnec.pt

Aviso legal

As opiniões manifestadas na Revista Portuguesa de Engenharia de Estruturas são da exclusiva responsabilidade dos seus autores.

Legal notice

The views expressed in the Portuguese Journal of Structural Engineering are the sole responsibility of the authors.

MASSENA, Beatriz [et al.] – Direct displacement-based design for RC structures – Procedure, advantages and shortcomings. **Revista Portuguesa de Engenharia de Estruturas**. Ed. LNEC. Série III. n.º 6. ISSN 2183-8488. (março 2018) 67-88.

1 Introduction

In the early nineties, the Performance-Based Seismic Engineering (PBSE) principles have been introduced in the seismic design of structures. Several authors [1, 2 and 3] have identified the limitations of traditional force-based design (FBD) procedures widespread in most of the design codes around the world to accomplish the PBSE requirements.

As the importance of displacements, rather than strength, has come to be better appreciated, the initial force based design procedures purely based on strength considerations were gradually modified to include consideration of displacements, the so-called “Modified Force-Based Design Methods” [3]. In these methods, most widespread in various seismic design codes of practice around the world, the design process is still carried out in terms of required strength and displacement capacity; with the Modified Force-Based Design Methods it is possible only to guarantee that a specified performance level is achieved, and no attempt is made to obtain a uniformity of risk of structural or non-structural damage.

Some researchers started pointing out this inconsistency, proposing displacement-based approaches for earthquake engineering evaluation and design. Several contributions [3] were made towards the development of Displacement-Based Design (DBD) approaches, but it was only in the 90’s that formal proposals were made to implement the emerging ideas into formalized design procedures. A state-of-art report was issued on this topic [4]. Sullivan *et al.* [5] carried out a comparative study of displacement-based design methods to evaluate their limitations and performance and pointed out that the Direct Displacement-Based Design (DDBD) method, which was developed according to of Priestley works [3 and 6], is one of the most promising approaches. In comparison with other displacement-based design methods, DDBD is a relatively fast and simple method that designs a structure to satisfy a pre-defined drift level. The method requires in general little or no iteration to design a structure to achieve a specified displacement profile.

Priestley [2] proposed the concept of DDBD with the aim of mitigating the fundamental shortcomings in current force-based design (FBD) methods. The central idea of the DDBD procedure is to design the structures using as input the desired displacements to be sustained under the design seismic intensity.

The DDBD is based on the substitute structure concept proposed by Shibata and Sozen [7] for MDOF reinforced concrete (RC) structures based on the work developed by Gulkan and Sozen [8], which represents the nonlinear structure with a substitute structure characterized by the secant stiffness corresponding to the maximum displacement response and by equivalent viscous damping representing the combined effects of elastic and hysteretic damping. This method is very simple to be applied and it is possible to use the familiar elastic response spectrum.

Sozen [9] and Moehle [10] carried out numerical and experimental studies of planar frames of mid-rise height indicating that displacement response is dominated by response in an apparent first mode. Saiidi and Sozen [11] demonstrated that this predominant component of the displacement response could be modelled using a single-degree-of-freedom (SDOF) oscillator having hysteretic

properties similar to those of the constituent elements of the frame. These findings suggested that the global displacement of multistorey system may be estimated using simplified response spectrum methods. Numerous case studies confirm this view [10, 12 and 13]. Based on these outcomes Moehle [14] proposed a displacement-based design procedure for RC structures. This approach is based on expected structural displacements directly for evaluation of behavior of structural and nonstructural elements.

Kowalsky *et al.* [15 and 16] developed the DDBD procedure for SDOF structures (concrete bridge piers), by inverting the seismic design procedure. In the beginning of the process, a maximum target displacement is established and the required strength and stiffness are obtained. Afterwards, the procedure was developed for multi-span reinforced concrete bridges [17, 18, 19 and 20].

Calvi and Pavese [21] illustrated the conceptual formulation of DDBD applied to RC buildings, and then the procedure was developed for multi-story concrete building frames [22, 23, 24, 25, 26, 27, 28, 29 and 30]. Pettinga and Priestley [31] developed and verified a series of adjustments to the DDBD method, including improved design displacement profiles and equivalent lateral force distributions. A design drift reduction factor was introduced to account for higher-mode of vibration in drifts in taller frames. Sullivan *et al.* [32] developed the DDBD method for RC frame-wall structures and in 2007 Priestley *et al.* [30] developed a text book regarding the Displacement-Based Seismic Design of Structures.

Some authors investigated the application of the DDBD method and proposed some adaptations and other authors investigated the advantages and validated the DDBD method. Some references of these works can be found in [33].

From this literature review, DDBD appears as an evidence for what regards research. In order to implement this new design philosophy in the practical seismic design of structures, Calvi *et al.* [34] and Sullivan *et al.* [34 and 35] proposed the development of a model code for displacement-based seismic design. A research line of the RELUIS project, in Italy, undertook the work.

Powell [36] has pointed out the importance of implementing the DDBD procedure in computer programs and Sullivan *et al.* [37] proposed the development of the DBDSOFT for the application of DDBD to regular RC buildings. This program [38] relies on the user to indicate how the design solution should be developed; i.e. in this software the strength and stiffness of elements are not specified since they should be an outcome of the design process. Moreover, users of DBDSOFT assign strength proportions to plastic hinge locations and then equilibrium analyses are undertaken to arrive at required design strengths, in line with the DDBD approach. After the definition of the proportions of strength, the software computes the required design base shear and the required flexural strengths of the plastic hinge zones.

Sullivan [38] focuses on the advantages of including new analysis methods for Performance Base Design in future version of the Eurocode 8 [40] and Beyer [41] emphasizes the importance of introducing displacement-based design approaches in future versions of the Eurocode 8.

The purpose of this work is to investigate the direct displacement-

based seismic design approach in its globality. In particular, the emphasis is set herein on the definition of the equivalent viscous damping and on the concrete impact of choosing one or another expression of the equivalent damping on the resulting seismic design. Then, the efficiency of applying DDBD to RC plane frames and dual frame-wall structures is assessed. In this context, a detailed description of all the steps of the DDBD procedure is provided. It is also compared to the traditional force-based design (FBD). Particularly, the consequences of using the linear response spectrum suggested in the Eurocode 8 as input data is analyzed for all the case-studies. The main results are presented and discussed, the conclusions are identified and some recommendations outlined.

2 DDBD method for reinforced concrete structures

The DDBD is a simple design approach where the multi-degree-of-freedom (MDOF) structure is characterized by the secant stiffness associated with the maximum displacement and by a level of equivalent viscous damping of an equivalent SDOF structure. The characterization of the structure by secant stiffness avoids the many problems inherent in force-based design where initial stiffness is used to determine an elastic period, and forces are distributed between members in proportion to elastic stiffness. Figure 1 presents schematically an approach to describe a building structure (MDOF system) in terms of a SDOF, as presented by Calvi and Kingsley [42] for MDOF bridge structures, where is shown the required variables in DDBD procedure.

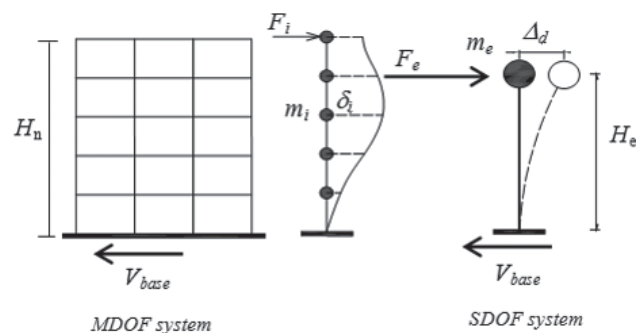


Figure 1 Simplified model of a multi-story building (adapted from [42])

2.1 DDBD for frames

The step-by-step DDBD procedure for RC frames is described in the following:

Step 1: Definition of the target displacement shape and amplitude of the MDOF structure on the basis of performance level considerations (material strain or drift limits) and then derive from there the design displacement Δ_d of the substitute SDOF structure of the MDOF.

The design story displacements Δ_i of the individual masses are obtained from:

$$\Delta_i = \omega_{\theta} \cdot \Delta_{i,ls} \quad (1)$$

where $\Delta_{i,ls}$ is the design displacement profile corresponding to the inelastic first mode shape at the design drift limit and ω_{θ} is the higher mode reduction factor and could be obtained by means of rational analysis or from the curves presented in Figure 2 according to Model Code [34].

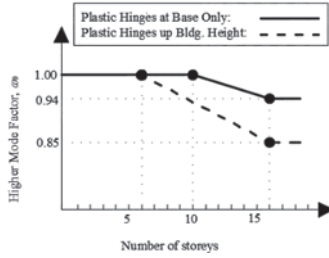


Figure 2 Higher mode reduction factor ω_{θ} [adapted from [34]]

According to Priestley *et al.* [30], the design story displacements for frame buildings will normally be governed by drift limits in the lower storey of the building (first storey).

The design displacement profile is given by:

$$\text{for } n \leq 4 \quad \Delta_{i,ls} = \theta_c H_i \quad (2)$$

$$\text{for } n > 4 \quad \Delta_{i,ls} = \theta_c H_i \frac{(4H_n - H_i)}{4H_n - h_n} \quad (3)$$

where H_i is the height of each story, H_n is the total height of the building (n stands for the number of the stories) and θ_c is the drift limit. Model Code [34] provides guidance as to when a structural system is expected to respond elastically the displaced shape should correspond to the fundamental mode shape obtained through eigenvalues analyses.

The equivalent design displacement can be evaluated as:

$$\Delta_d = \sqrt{\sum_{i=1}^n (m_i \Delta_i^2)} / \sum_{i=1}^n (m_i \Delta_i) \quad (4)$$

The mass of the substitute structure m_e and the effective height H_e are given by the following equations:

$$m_e = \sum_{i=1}^n m_i \left(\frac{\Delta_i}{\Delta_d} \right) = \frac{\sum_{i=1}^n m_i \Delta_i}{\Delta_d} \quad (5)$$

$$H_e = \frac{\sum_{i=1}^n (m_i \Delta_i H_i)}{\sum_{i=1}^n (m_i \Delta_i)} \quad (6)$$

Step 2: Estimation of the level of equivalent viscous damping ξ_{eq} . Several equations proposed in the technical literature [30] can be used to evaluate the equivalent viscous damping (this subject is discussed in Section 3). To obtain the equivalent viscous damping the displacement ductility μ must be known (Eq. 7). The displacement ductility is the ratio between the equivalent design displacement and the equivalent yield displacement Δ_y (see Eq. 7 and Figure 3).

$$\mu = \frac{\Delta_d}{\Delta_y} \quad (7)$$

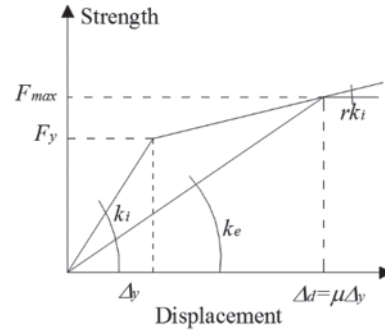


Figure 3 Constitutive law of the equivalent SDOF system

The equivalent yield displacement is estimated according to the considered properties of the structural elements, for example with approximated equations proposed by Priestley *et al.* [30], and based on the yield drift θ_y :

$$\Delta_y = \theta_y H_e \quad (8)$$

θ_{yx} is the yield drift for a given bay x as:

$$\theta_{yx} = 0.5 \varepsilon_y L_{b,x} / h_{b,x} \quad (9)$$

where ε_y is the yield strain of steel, $L_{b,x}$ is the beam length of span x and $h_{b,x}$ is the beam section depth of beam x .

For frames that possess bays with different lengths the yield drift can be computed as:

$$\theta_{y,i} = \sum_{j=1}^{nb} M_{x,j} \theta_{yx} / M_{frame,i} \quad (10)$$

where M_x is the proportion of bending moment of each bay, M_{frame} is the proportion of bending moment of frame i . To account for the inelastic behaviour of the real structure, the hysteretic damping (ξ_{hyst}) is combined with elastic damping (ξ_0). Usually, for RC structures the elastic damping is taken equal to 0.05, related to critical damping.

The equivalent viscous damping of the substitute structure for RC frames could be defined according to Priestley *et al.* [30] by the following equation:

$$\xi_{eq} = 0.05 + 0.565 \left(\frac{\mu - 1}{\mu \pi} \right) \quad (11)$$

The global damping could be computed, as an alternative by the weighted average as:

$$\xi_{eq} = \frac{\sum_{i=1}^n \xi_i V_i \theta_i}{\sum_{i=1}^n V_i \theta_i} \quad (12)$$

where, ξ_i is the damping at level i , based on the drift ductility at that level, defined as:

$$\mu_i = \theta_i / \theta_{yi} \quad (13)$$

θ_i is the design story drift and θ_{yi} is the story yield drift. V_i is the absolute value of story shear.

Step 3: Determination of the effective period T_e of the SDOF structure. The effective period of the SDOF structure at peak displacement response is found from the design displacement spectrum for the equivalent viscous damping ξ_{eq} , i.e. entering the design displacement of the substitute SDOF structure Δ_d and determining the effective period T_e (see Figure 4 a) and Eq. (14)).

$$T_e = \frac{\Delta_d}{\Delta_{D,\xi}} T_D \quad (14)$$

where T_D is the spectral displacement corner period and $\Delta_{D,\xi}$ is the spectral displacement demand at this period for the anticipated level of equivalent viscous damping and could be found from the formulation defined in the Eurocode 8 [40], as:

$$\Delta_{D,\xi} = \Delta_{D,eI} \eta \quad (15)$$

where η is the damping correction factor and could be determined by the expression:

$$\eta = \left(\frac{10}{5 + \xi_{eq}} \right)^{1/2} \quad (16)$$

The graphical approach shown in Figure 4 a) is valid for structures that have a design displacement Δ_d lower than the spectral displacement demand $\Delta_{D,\xi}$.

For cases when the design displacement (Δ_d) exceeds the $\Delta_{D,\xi}$, as presented in Figure 4 b), and according to the Model Code [34 and 35], the value of the effective period T_e should be defined in such a way that the corresponding effective stiffness is reduced, obtained by Eq. (17), and should not exceed the limit set on the effective stiffness given by Eq. (18).

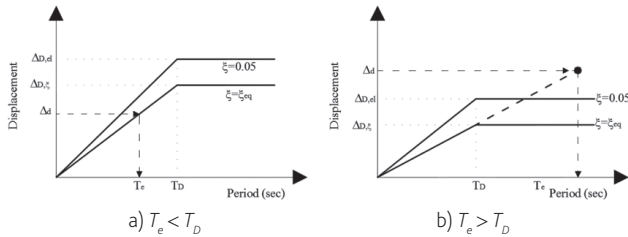


Figure 4 Design Displacement Response Spectrum (DRS) [adapted from [34]]

Step 4: Derivation of the effective stiffness k_e of the substitute structure from its effective mass and effective period, given by:

$$k_e = \frac{4\pi^2 m_e}{T_e^2} \quad (17)$$

$$k_{e,max} = \frac{4\pi^2 m_e}{T_e^2} \cdot \frac{\Delta_{D,\xi d}}{\Delta_d} \quad (18)$$

The design base shear V_{base} is the product of the equivalent SDOF system effective stiffness and the design displacement.

$$V_{base} = k_e \Delta_d \quad (19)$$

As suggested by Priestley *et al.* [30], the $P-\Delta$ effects should be included in DDBD. According to Model Code [34], to the design base shear obtained in the previous Eq. (19) should be added a $P-\Delta$ base shear component given as:

$$V_{P-\Delta} = C \frac{\sum_{i=1}^n P_i \Delta_i}{H_e} \quad (20)$$

where H_e is the equivalent height of the SDOF substitute structure obtained with Eq. (6) and C is a $P-\Delta$ parameter that should be obtained from rational analyses or taken as zero for structures with $m_e g / K_e H_e < 0.05$, 0.5 for RC buildings and 1.0 for steel structures.

A $P-\Delta$ stability index $\theta_{P-\Delta}$ - Eq. (21), where P is the axial force due to gravity loads, should be evaluated for each level of a building and should not exceed a limit of 0.3.

$$\theta_{P-\Delta,i} = \frac{P_i (\Delta_i - \Delta_{i-1})}{V_{di} (h_i - h_{i-1})} \quad (21)$$

The design base shear is then given by the following equation:

$$V_{base} = k_e \Delta_d + V_{P-\Delta} \leq 2.5 \cdot \eta \cdot PGA \cdot m_e + V_{P-\Delta} \quad (22)$$

If the Elastic Design Spectrum is defined according to Priestley *et al.* [30], a limit is set to the design base shear as a function of the peak ground acceleration (PGA). Furthermore, the Elastic Design Spectrum depicted in Figure 4 disregards the non-linear variation in displacements that would correspond to the Eurocode 8 [40] acceleration Design Response Spectrum in the range $0 \leq T \leq T_c$, taken herein as linear (see Figure 4).

After the evaluation of the required base shear force, it is distributed in height of the MDOF structure as inertia forces and from structural analysis (Step 5); the required moment capacity at plastic hinges is obtained, as described in Step 6.

Step 5: Distribution of the design base shear force V_{base} to the locations of story mass of the building (MDOF structure), as:

$$\text{for } n < 10 \quad F_i = V_{base} \frac{(m_i \Delta_i)}{\sum_{i=1}^n (m_i \Delta_i)} \quad (23)$$

$$\text{for } n \geq 10 \quad F_i = F_t + 0.9 V_{base} \frac{(m_i \Delta_i)}{\sum_{i=1}^n (m_i \Delta_i)} \quad (24)$$

where $F_t = 0.1 V_{base}$ at roof level, and $F_t = 0$ at all other story levels.

Step 6: Definition of moment capacities at potential hinge locations.

There are two different methods for defining the moment capacities at potential hinge locations for frames. One requires a conventional structural analysis and is based on the stiffness of structural members at expected design displacement response; the other is a simplified method based on equilibrium considerations (statically admissible distribution of internal forces) [33].

Step 7: Capacity design requirements for frames.

Capacity design rules are required to ensure that plastic hinges cannot develop at unintended locations and only for the desired mechanism.

2.2 DDBD for dual-wall structures

The global response of a dual-wall system is a combination of both pure frame and wall building responses (see Figure 14, configuration 3). There are different dual systems configurations; the structural system could consist of boundary frames integrally linked to structural walls by moment-resisting beams or can consist of end walls and parallel one-way frames. Regardless the configuration of the dual system, the dynamic performance is significantly different from that of a pure frame or wall building structure due to the interaction that take place between the structures. Figure 5 shows a flowchart of the DDBD procedure for dual-wall structures until the calculation of the design base shear.

In Figure 5 β_f represents the fraction of base shear force carried by the frames. It may be decided based on engineering judgment; however, as suggested by [30], the total base shear V_f carried by frames could be settled between 20% and 60% of the total base shear V_{base} .

3 Investigations on the equivalent viscous damping in direct displacement-based design

From the step-by-step procedure of DDBD methodology the estimation of the equivalent viscous damping can be seen as a crucial point of the procedure. A wrong assessment of this parameter can possibly lead to important errors on the actual ductility demand of the structural elements.

A study [33] is carried to assess these formulas and to provide information on the impact of the choice of one or another formulation on the seismic design. It is more precisely focused on the proposals of Dwairi-Kowalsky [43], Eq. (25), and Blandon-Priestley [44], Eq. (26) and Eq. (27).

$$\xi_{eq} = \xi_0 + \frac{a}{\pi} \left(1 - \frac{1}{\mu^b} \right) \cdot \left(1 + \frac{1}{(T_e + c)^d} \right) \cdot \frac{1}{N} \quad (25)$$

$$N = 1 + \frac{1}{(0.5 + c)^d}$$

(Large and narrow Takeda)

$$\xi_{eq} = \xi_0 + C_{LT} \left(\frac{\mu - 1}{\pi \mu} \right) \% \quad (26)$$

$$C_{LT} = 65 + 50(1 - T_{eff}) \quad T_e < 1s$$

$$C_{LT} = 65 \quad T_e \geq 1s$$

(Large Takeda)

$$\xi_{eq} = \xi_0 + C_{ST} \left(\frac{\mu - 1}{\pi \mu} \right) \% \quad (27)$$

$$C_{ST} = 50 + 40(1 - T_{eff}) \quad T_e < 1s$$

$$C_{ST} = 50 \quad T_e \geq 1s$$

(Narrow Takeda)

3.1 Assessment of existing formulas

As above mentioned, a study was carried out to assess the existing formulas. Thus, to be used for comparison and assessment purposes, a full set of SDOF systems are defined, for which the effective period, the maximum displacement and the ductility level are known and consistent. The main governing parameters of these simple systems are given on Figure 3. As the focus is essentially on the hysteretic behavior, the viscous damping ξ_0 is assumed equal to zero.

The parameters of the different considered SDOF systems are calibrated in such a way that the average of the maximum displacement obtained by non-linear time-history analyses (NLTHA) is equal to the displacement Δ_d of Figure 3.

The methodology followed to determine the SDOF properties, derived from a similar study proposed by Blandon and Priestley [44], is the following:

- 1) Choose a specific T_e , a given value of the post-yield ratio r and a given ductility μ . In this study, r is always considered equal to 0.05;
- 2) Make a first arbitrary guess of the displacement Δ_d . This initial guess is made according to the Priestley [29] formula for equivalent damping [33]. The displacement can then be estimated from this value of equivalent damping and from the elastic displacement response spectrum;
- 3) Knowing T_e , m_e , μ , r and Δ_d , the whole constitutive law is then defined;
- 4) A series of nonlinear time-history analyses (NLTHA) of the SDOF system are performed for different ground motions. The maximum displacement obtained for each NLTHA is recorded. The average of these maximum displacements is compared to the assumed value of Δ_d . If the difference between the assumed value and the average results is less than 0.5%, the characteristics of the SDOF system are stored, otherwise the numerical average displacement is used as a new guess of the displacement and the process starts again at step 3 with a new definition of the constitutive law.

The non-linear dynamic analyses are performed partly with Seismostruct [45], partly with Finelg [46]. Six groups of SDOF systems are defined according to the type of assumed hysteretic behavior (large or narrow Takeda model as shown in Figure 6) and to the type of ground motion time-history. The Takeda Model is used to represent the non-linear behavior of concrete structures and structural members. The narrow Takeda model ($\alpha = 0.5$ and $\beta = 0$) is generally assumed suitable for columns and walls and the large Takeda model ($\alpha = 0.3$ and $\beta = 0.6$) for RC beams and frames [47].

Three series of ground motions are first considered:

- The first series (series I) is a set of 10 accelerograms including the 5 synthetic accelerograms used by Blandon and Priestley for the calibration of their equivalent damping formula [44] and five new generated accelerograms. The current set of 10 accelerograms corresponds to a reference displacement spectrum more or less linear up to a corner period equal to 4s, with a PGA equal to 0.7g.

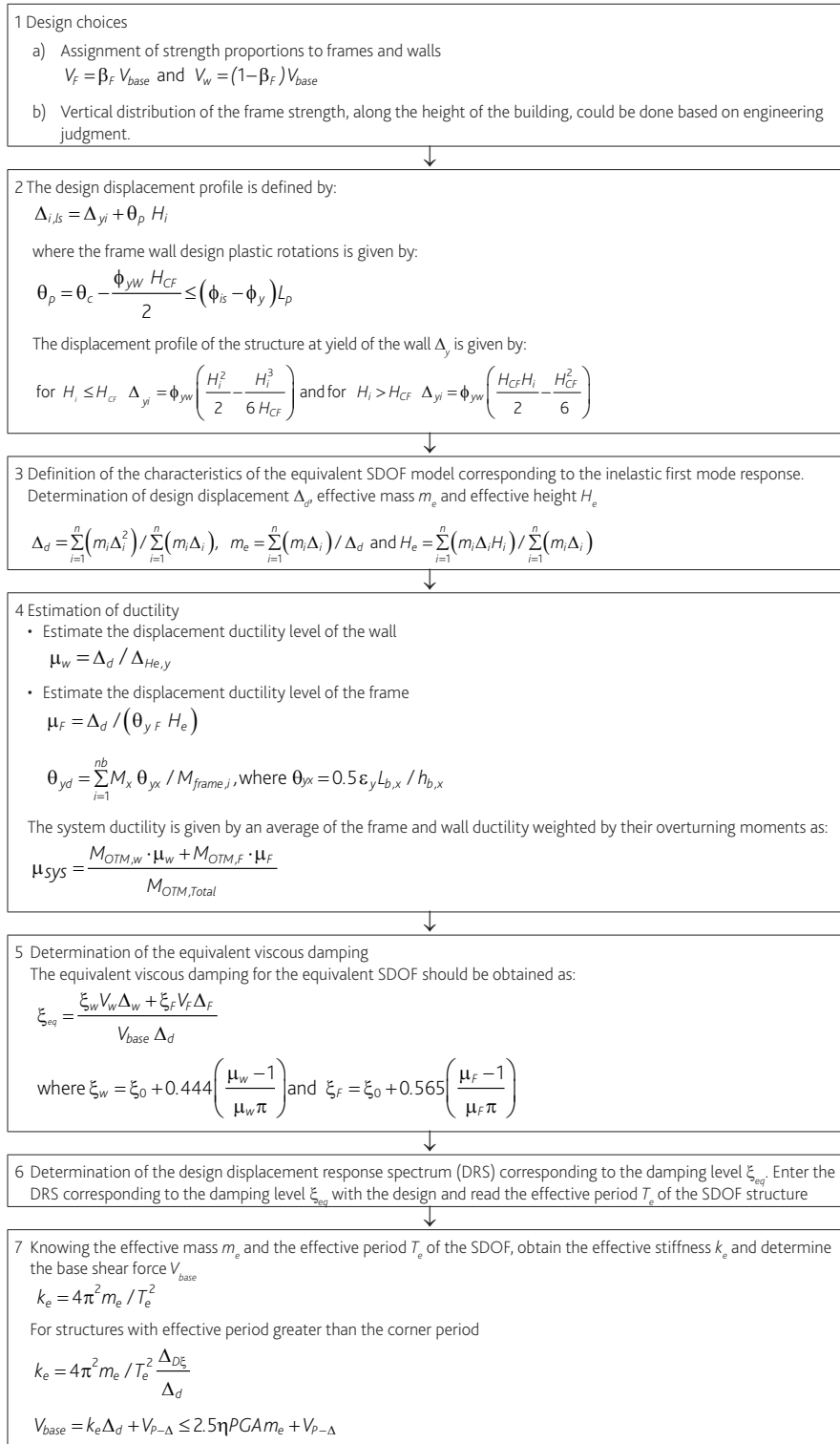


Figure 5 Flowchart of the DDBD for dual-wall structures (adapted from [35])

- The second series (series II) is a set of 10 artificially generated accelerograms with a spectrum compatible with a type 1 spectrum of the Eurocode 8, with a PGA equal to 0.7g.
- The third series (series III) is a set of 10 artificially generated accelerograms with a spectrum compatible with a type 2 spectrum of the Eurocode 8, with a PGA equal to 0.5g.

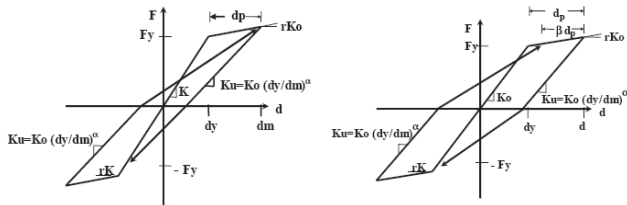


Figure 6 Takeda model [adapted from Blandon [44]]

Series III is considered only in order to be exhaustive with respect to the Eurocode 8. Indeed, a displacement spectrum exhibiting a corner period of 1.2 s is obviously unrealistic and unsafe, even if this value is the default value proposed by the Eurocode 8 for type 2 spectrum. To this purpose, it is interesting to refer to [48], where it is clearly stated that the corner period should be related to the earthquake magnitude and that the range of variation should be somewhere between 4 and 12 s, which leads to the conclusion that Eurocode seems to be clearly unsafe even for type 1 for what regards displacement spectra, since the proposed value for T_D is equal to 2 s. It is also of interest to notice that, in the Portuguese National Annex to the Eurocode 8, it is proposed to consider a corner period equal to 2 s for both type 1 and type 2 spectra. Thus, even if the results obtained with series III are fully presented in this work, it must be noticed that they are much less relevant than those corresponding to series I and II, with corner period T_D respectively equal to 2 and 4 s. Figure 7 represents, for each of the first three series, the reference displacement spectrum (herein call as theoretical spectrum, i.e. a linear function of the effective period up to the corner period T_D followed by a horizontal plateau) and the average response spectrum obtained from the selected accelerograms by linear time-history analysis (LTHA) with a viscous damping of 5%. Accelerograms of series II and III were generated with the GOSCA software [49].

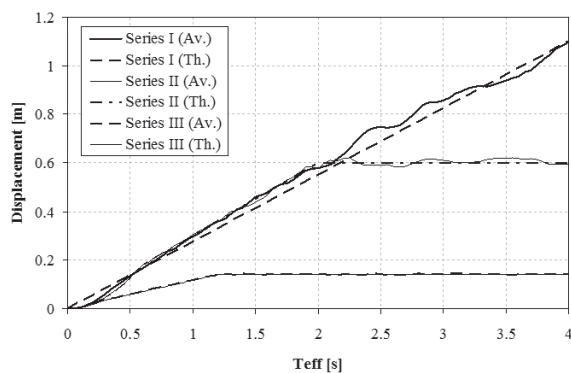


Figure 7 Reference displacement spectrum (Th.) and average numerical spectrum (Av.) for each series

As an example, Figure 8 presents the target displacement obtained for effective periods ranging from 0.5s to 3.5s and ductility ranging from 2 to 6 with the first series of accelerograms, respectively for narrow and large Takeda hysteretic model. The curves plotted on these figures can be considered as inelastic displacement spectrum expressed as a function of the effective period, i.e. associated with the period related to the secant stiffness corresponding to the maximum expected displacement.

Figures show a general trend to decreasing displacements when the ductility increases, due to a greater amount of energy dissipated in the hysteretic cycles. Further, for similar effective period and ductility, the maximum displacement obtained with the large Takeda model is smaller than the one obtained with the narrow Takeda model, which is again due to the greater amount of energy dissipated in the former model. The whole set of results obtained for the 3 series can be found in [33].

From these numerical displacements, it is then possible to evaluate an equivalent viscous damping level for each configuration (i.e. for each couple $T_e - \mu$). This is done numerically by computing, by means of linear time-history analyses, the average elastic displacement spectrum for each series of ground motion and for different level of viscous damping (varying from 0 to 40%), and by selecting the viscous damping level that provides an average spectral displacement equal to the maximum displacement of the NLTHA. These values of equivalent damping ξ_{eq} are presented on Figure 9 for the first series.

The whole set of results (available in Ref. [33]) can then be used to assess the recent proposals of Blandon-Priestley (B-P) and Dwairi-Kowalsky (D-K). Figure 10 compares the relative difference between the equivalent damping obtained from the numerical results and from the B-P and D-K formulas. The comparison is done for both narrow and large Takeda hysteretic models and for the 3 series of ground motion.

Even if it is difficult to draw general conclusions from such a small sample of ground motion, some general tendencies can be observed:

- The average relative error between numerical results on one hand and approximated results (B-P and D-K) on the other hand tends to diminish when ductility increases. This means that damping tends towards underestimated values for higher ductility level.
- A slight tendency for a decreasing error can be observed when effective period increases.
- For series 2 and 3, a very important overestimation of the damping level is observed for effective periods greater than the corner period of the displacement spectrum.
- For low ductility level, B-P approach leads to higher values of damping than D-K approach, while the tendency is inverted for high ductility level.
- Except for very short effective periods (0.5s), for periods greater than the corner and for some specific cases of low ductility, the absolute value of the relative error between numerical results and results obtained from the formulas is always under 25%.

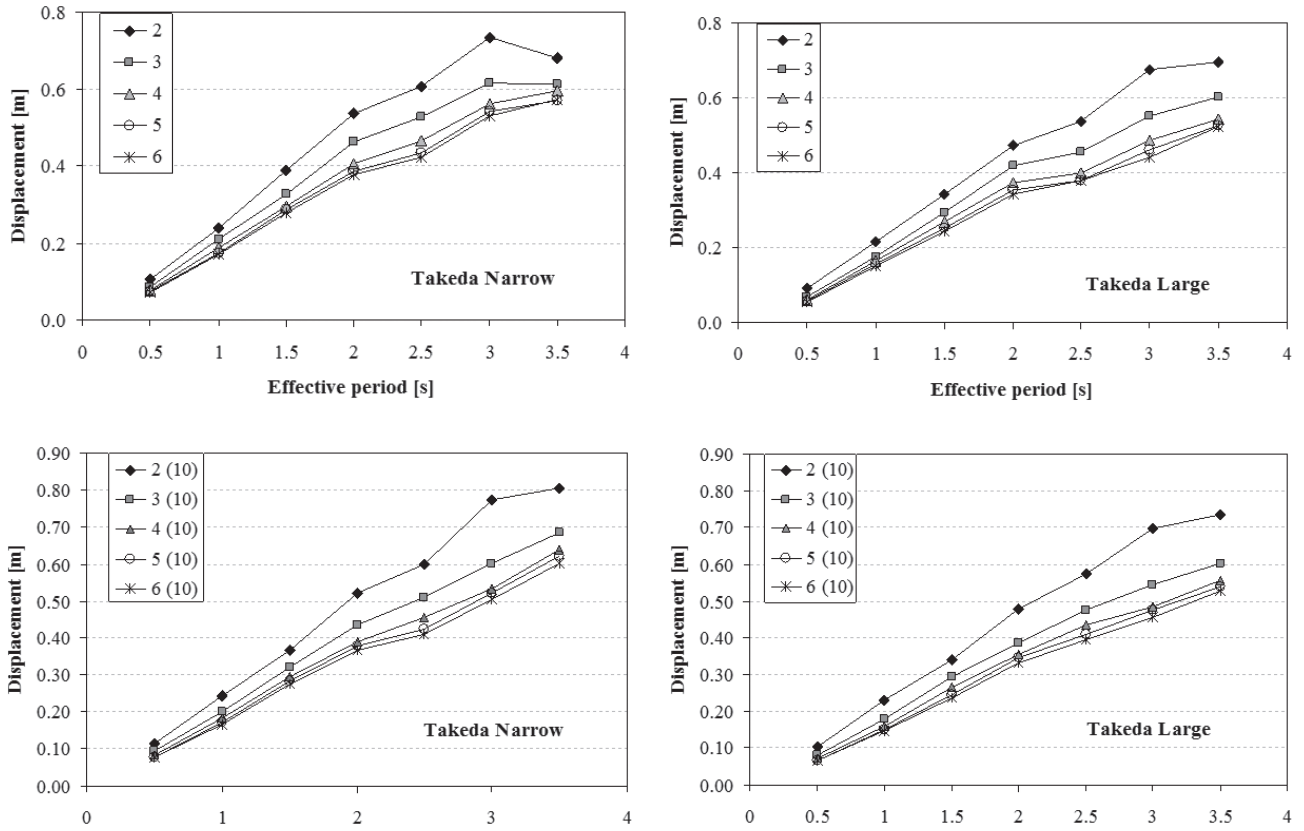


Figure 8 Displacement as a function of the effective period for different ductility level (1st series)

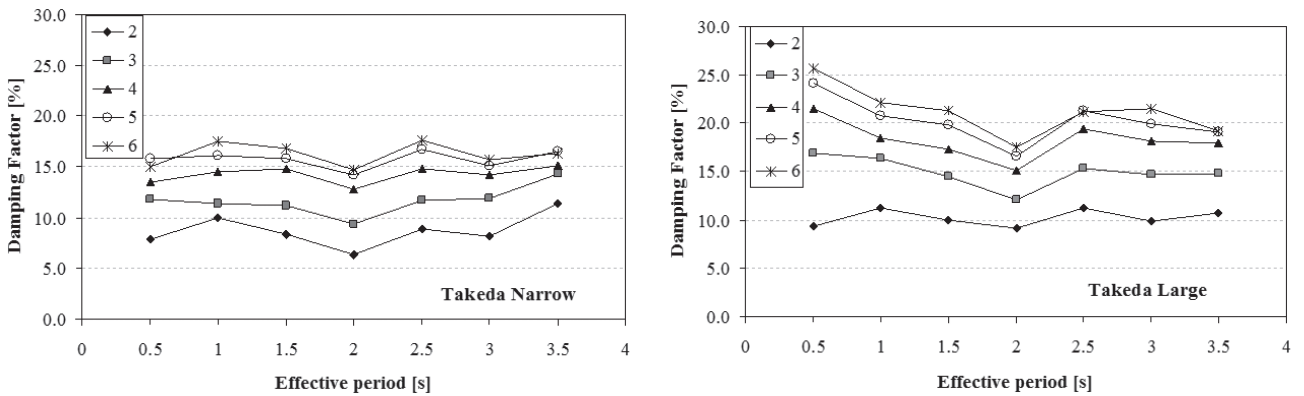


Figure 9 Equivalent damping obtained from the numerical results function of T_e (1st series)

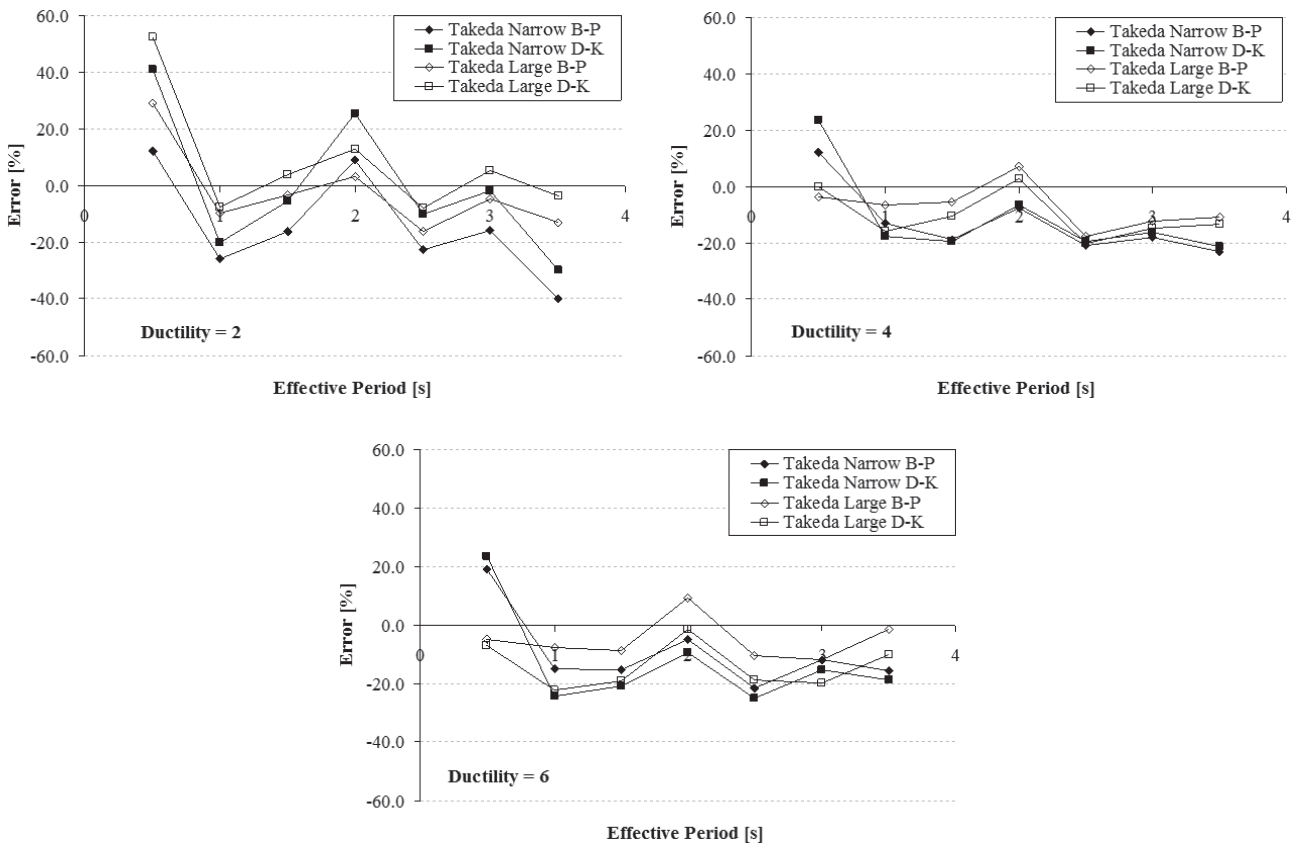


Figure 10 Relative error on the displacement $[(Dep_{formula} - Dep_{num}) / Dep_{num}]$ in % as a function of T_e (1st series)

3.2 Influence of the choice of equivalent damping formulation on the resulting design

In the DDBD context, the equivalent damping is not the final objective, but only a tool to define the characteristics of the designed system (effective period, stiffness, base shear) for a given value of the target displacement. To study the problem from this point of view, an example of design of a single circular bridge pile adapted from Priestley [20] is used (see Figure 11). The designed pile is then subjected to a series of NLTHA and the ductility assumed for the design is compared to the actual ductility demand.

The yield displacement Δ_y of the pile is given by Eq. (28). No drift limit is considered, to allow for any ductility without being limited by the overall rotation of the system.

$$\Delta_y = 2.35 \epsilon_y H^2 / 3d \quad (28)$$

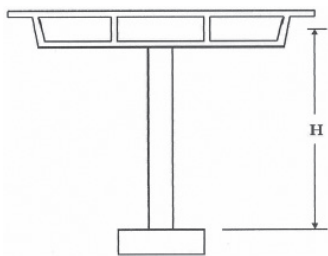
Three design situations are considered:

- Case 1: design on the base of the theoretical spectrum (i.e. a linear function of the effective period) corresponding to the first series of accelerograms considered in the previous section of the paper (see Series I in Figure 7), assuming a narrow Takeda hysteretic behavior of the pile, which is the one recommended for columns;

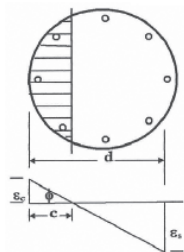
- Case 2: design on the base of the average spectrum computed from the 6 accelerograms of the first series, with a narrow Takeda hysteretic behavior. In this case, the only source of difference between the assumed ductility and the actual ductility of the system would only be the coarse estimation of the equivalent damping, while in case 1, another possible source is the difference between the theoretical spectrum used for the design and the actual spectrum corresponding to the accelerograms used for the assessment;
- Case 3: design on the base of the theoretical spectrum corresponding to the first series of accelerograms, but assuming a large Takeda hysteretic behavior, which is less realistic for a pile, but allows a comparison between different approaches proposed to relate the equivalent damping with the type of dissipative behavior.

The diameter and height of the pile are defined to target specific values of the effective period and of the design ductility, even if some of the resulting configurations may not be very representative of practical situations. The design is performed according to the formulas proposed by Priestley [3], Blandon - Priestley [44] and Dwairi-Kowalsky [43] and the resulting effective period for each situation are presented in Table II.

In all cases, Priestley formula (derived on the base of sinusoidal ground motion) leads to higher effective periods than the other two formulas and, in general, B-P and D-K approaches lead to very close values of the effective period, except for low ductility level, where D-K approach produces slightly higher values. It is also interesting to note that, when the effective period is higher, the effective stiffness and hence the design base shear are decreasing consequently.



(a) Cantilever bridge columns



(b) Column section and Limit State Strains

Figure 11 Typical geometry of the example (single pile) adopted from [20]

The resulting SDOF systems are then submitted to the accelerograms of the first series. The average actual ductility demand obtained from NLTHA is presented in Figure 12 for the different damping equations. Figure 13 emphasizes the comparison between the 3 approaches for design case 2.

From these figures, it can be observed that for an assumed ductility level equal to 2, the systems designed according to all 3 approaches exhibit an actual ductility in close agreement with the assumed ductility. On the other hand, for an assumed ductility equal to 4 or 6, the actual ductility of the systems designed according to B-P or D-K approaches is smaller than the value assumed for the design. Moreover, for Priestley approach, the actual ductility demand is closer to the assumed value, but can in some cases exceed this value. Added to the fact that the design base shear is smaller following Priestley approach than following B-P or D-K approaches, it can be stated that B-P and D-K formulas lead to a safe design since the actual ductility demand will never exceed the ductility assumed for the design and since the level of design base shear is higher.

To assess B-P and D-K equations, Table III presents three different procedures for comparing the actual ductility demands. Firstly, it compares the actual ductility demands obtained for systems designed for the same design conditions (case 1 and case 2 respectively) but using either B-P or D-K equation for the estimation of the equivalent damping. Secondly it compares the actual ductility

demands obtained with the same equivalent damping definition (B-P and D-K respectively) but with a displacement spectrum being either the theoretical one or the exact spectrum obtained for the selected accelerograms used for the NLTHA assessment. Finally the third one compares the actual ductility demands obtained with the same equivalent damping definition (B-P and D-K respectively) but corresponding to different hysteretic models (narrow or large Takeda). The main outcome of this comparison is that the average difference resulting from the choice of either B-P or D-K equation, and even from the choice of either a narrow or a large Takeda hysteretic model, is smaller than the average difference resulting from the use of either a theoretical spectrum or a real one.

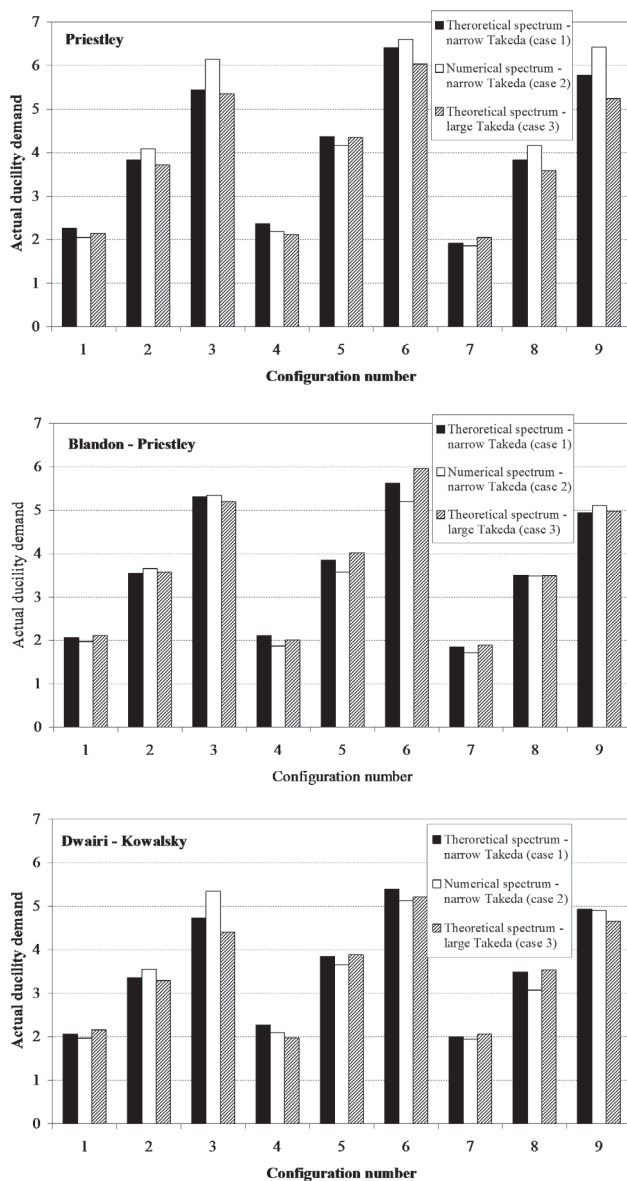


Figure 12 Results of the NLTHA assessment of the designed piles – average actual ductility

Table I Main characteristics of the pile

Configuration number	Diameter [m]	Height [m]	Elastic displacement [m]	Design ductility	Design displacement [m]
1	1.50	10	0.118	2	0.235
2	2.10	7.5	0.047	4	0.189
3	1.50	5	0.029	6	0.176
4	1.75	15	0.227	2	0.453
5	1.90	10	0.093	4	0.371
6	1.90	8	0.059	6	0.356
7	1.90	20	0.371	2	0.742
8	1.80	12	0.141	4	0.564
9	2.00	10	0.088	6	0.529

Table II Effective period obtained for the different configurations

Case 1 (Takeda narrow – design spectrum)			Case 2 (Takeda narrow – numerical spectrum)			Case 3 (Takeda large – design spectrum)		
T_{eff} [s] Priestley	T_{eff} [s] Blandon-Priestley	T_{eff} [s] Dwairi-Kowalsky	T_{eff} [s] Priestley	T_{eff} [s] Blandon-Priestley	T_{eff} [s] Dwairi-Kowalsky	T_{eff} [s] Priestley	T_{eff} [s] Blandon-Priestley	T_{eff} [s] Dwairi-Kowalsky
1.04	0.98	1.00	0.98	0.93	0.96	1.12	1.08	1.09
1.01	0.95	0.92	1.02	0.96	0.95	1.10	1.05	1.02
1.00	0.94	0.89	1.04	0.97	0.94	1.10	1.05	0.96
2.00	1.86	1.94	1.81	1.67	1.75	2.17	2.04	1.97
1.98	1.81	1.81	1.92	1.72	1.74	2.16	2.03	2.00
2.02	1.84	1.81	2.18	1.78	1.74	2.22	2.08	2.00
3.02	2.80	2.94	3.47	2.74	3.00	3.55	3.34	3.45
3.00	2.74	2.76	3.38	2.77	2.71	3.29	3.07	3.03
3.00	2.74	2.78	3.42	2.80	2.71	3.30	3.07	2.96

Table III Relative difference on the actual ductility demand between (i) B-P and D-K for the same design case, (ii) Case 1 and Case 2 for the same approach, (iii) Case 1 and Case 3 for the same approach [in %]

Configuration	B-P / D-K		Case 1 / Case 2		Case 1 / Case 3	
	Case 1	Case 2	B-P	D-K	B-P	D-K
1	-0.1	0.1	4.5	4.8	-2.3	-4.5
2	5.5	2.9	-2.9	-5.4	-0.9	2.0
3	12.2	0.1	-0.8	-11.5	1.9	7.3
4	-7.2	-10.6	12.9	8.8	4.9	15.3
5	-0.2	-2.0	7.2	5.3	-4.5	-0.8
6	4.4	1.5	8.2	5.3	-5.7	3.4
7	-7.1	-11.8	7.8	2.3	-1.9	-3.3
8	0.4	13.5	0.5	13.7	0.1	-1.3
9	0.3	4.1	-3.2	0.5	-0.7	5.8
average	0.9	-0.2	3.8	2.6	-1.0	2.6

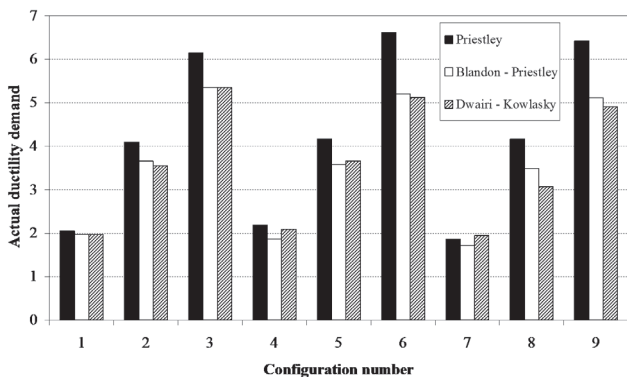


Figure 13 Results of the NLTHA for case 2 (design based on the average spectrum) – average ductility demand

3.3 Discussion

In section 3 an illustrative comparison was performed between the equivalent damping obtained from numerical NLTHA for different types of ground motion and the equivalent damping obtained with two of the most recent theoretical formulations proposed in literature [33], respectively by Blandon-Priestley and Dwairi-Kowalsky. The main outcome of this comparison is that, except in some specific conditions that should require additional investigations (i.e. very small effective periods, effective periods greater than the corner period of the displacement response spectrum and some cases of low ductility), the different approaches lead to a rather important scattering of the results, but with a range of variation of the error between the damping values obtained from numerical and theoretical approaches around 25%.

Except in the specific conditions referred above, no significant difference in terms of accuracy is evidenced between Dwairi-Kowalsky and Blandon-Priestley formulations. The consequences of choosing one or another damping equation on the design was investigated. It concludes that both Blandon-Priestley and Dwairi-Kowalsky approaches lead to an accurate design for small ductility and to a safe design, even if less accurate, for moderate to high assumed ductility. Further it appears impossible to determine if one of the two approaches is better than the other, as the difference in terms of accuracy related to the assumed shape of the design spectrum is much greater than the difference related to the choice of one or another viscous damping formulation. Therefore, it is thought that the choice between both formulations can be done according to the simplicity of the formulation, which gives an obvious advantage to Dwairi-Kowalsky proposal.

Priestley *et al.* (2007), based on Dwairi-Kowalsky equation (Eq. (25)) and on the work of Grant *et al.* [50], proposed simplified equations for the definition of equivalent damping for frames and walls (Eq. (25), Eq. (26) and Eq. (27), respectively). The study of Grant *et al.* [50] considered that (i) the period-dependency is insignificant for most rules for $T < 1$ sec and (ii) an elastic damping ratio of 5%. Thus, the coefficient C in Eq. (26) and Eq. (27) was adjusted in such way that final values are correct if the elastic damping ratio is 5%.

4 Application of the DDBD methodology to RC plane structures

In this section, a set of 3 plane RC systems (i.e. a vertically regular frame, a vertically irregular frame according to the Eurocode 8 [40] definition and a dual system) are designed according to the DDBD procedure and, with the aim of comparing procedures, to the traditional force-based design method (FBD). All structures designed are seismically assessed through nonlinear static (Pushover) and nonlinear dynamic time-history analyses, performed with Seismostruct [45] and results of both analyses are compared and discussed. Nonlinear static analyses are developed according to the N2 method, as suggested in the Eurocode 8. Nonlinear dynamic analyses are performed using a group of seven accelerograms, generated with the GOSCA software [49].

4.1 Description and design assumptions

The configurations of the RC plane structures under study, schematically presented in Figure 14, are defined based on the criterion for vertical regularity proposed in the Eurocode 8 part 1 Section 4.2.3.3. Configuration 1 is an eight-storey frame regular in elevation with three bays. Configuration 2 is similar to Configuration 1 and characterized by vertical irregularity, likely to induce a ground soft-storey plastic mechanism (first floor with 5 m height). Configuration 3 is a regular eight-storey RC plane frame-wall structure, consisting in a single RC plane frame regular in elevation coupled in the same plane with a RC wall.

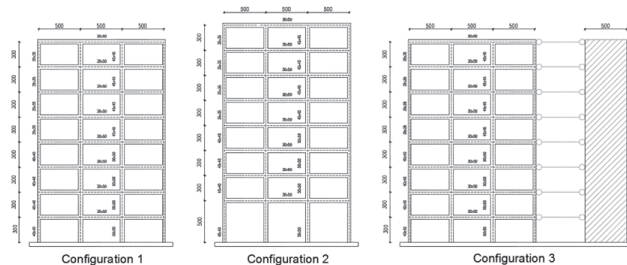


Figure 14 Plane structures under study – length and cross sections of the structural elements [dimension in cm]

In addition to the self-weight of the beams and the slab, a distributed dead load of 2 kN/m² due to floor finishing and partitions is considered, as well as an imposed live load with nominal value of 2 kN/m². The slab thickness is equal to 0.15 m and its contribution to the structural response was taken in account by considering an effective beam width as proposed in the Eurocode 8 [40], Section 5.4.3.1.1. The column cross sections are defined (see Figure 14), in order to limit the normalized axial force [40]. For the DDBD procedure, an overall drift limit (θ_c) of 2.5% for configuration 1 and 2 and 2.0% for configuration 3 are respectively considered, in accordance with the DDBD Model Code [35] suggestion. The soil-foundation-structure interaction is not taken into account. The bases of the columns are assumed to be fixed. For the seismic load combination, dead loads are considered with their nominal value and live loads as 30% of their nominal value.

According to the results achieved and the discussion presented in section 3, for the definition of equivalent damping for RC frames and walls, Eq. (29) and Eq. (30), respectively – are the ones used in this work in the following sections:

$$\xi_{eq} = 0.05 + 0.565 \left(\frac{\mu - 1}{\pi \mu} \right) \quad (29)$$

$$\xi_{eq} = 0.05 + 0.444 \left(\frac{\mu - 1}{\pi \mu} \right) \quad (30)$$

4.2 Seismic action

The buildings set is considered being in Portugal (Algarve) as an ordinary building class of importance II ($\gamma_I = 1.0$ for ordinary buildings). The seismic action is defined according to the Eurocode 8 and the Portuguese National Annex [51] with the elastic acceleration response spectrum S_a for subsoil class D. The design ground acceleration a_g used in the definition of the response spectrum was 0.25 g. The elastic 5% damped displacement spectrum S_{De} used for DDBD is characterized by a corner period of 2 sec. Figure 15 shows, as an example, one of the seven accelerograms generated with the GOSCA program [49] and used in the nonlinear dynamic time-history analyses. Figure 16 shows the corresponding response spectra in acceleration and displacement.

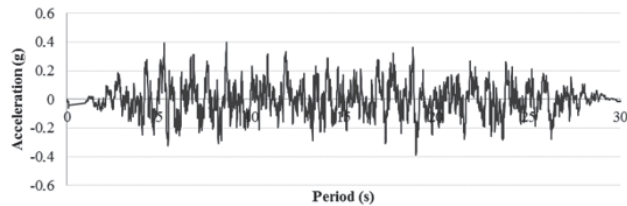


Figure 15 Accelerogram generated with the software GOSCA

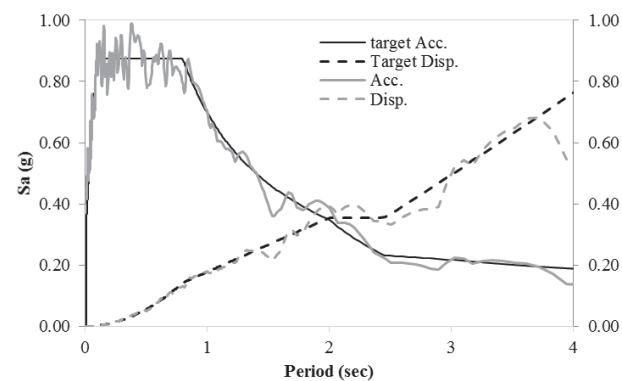


Figure 16 Reference and corresponding Elastic Acceleration and Displacement Response Spectrum

4.3 Design

The DDBD and FBD procedures are applied to RC plane structures described previously. Table IV and Table V show the main design

parameters related with DDBD procedure up to the definition of the base shear for RC plane frame-wall structure for different fractions of the total base shear supported by the frame, β_F (i.e. $\beta_F = 0.40, 0.50$ and 0.60).

Regarding the DDBD procedure for frame structures, the required flexural strength of beams was obtained by means of equilibrium considerations and for columns a simple procedure was adopted as suggested by Priestley *et al.* [30], considering central points of contra-flexure in each column. The simple procedure admitting the central points of contra-flexure in each column to obtain the required flexural strength of members is more straightforward than considering equilibrium considerations [33]. The design moment at the column base was assumed as $0.60 V_c H_1$, where V_c is the column shear and H_1 is the height of the first floor as suggested by Priestley *et al.* [29].

In [33], the DDBD procedure is described for regular plane frame-wall structures. Herein β_F was considered as 40%, 50% and 60%, respectively.

The FBD procedure is performed by linear dynamic response spectrum analysis where the behaviour factor ($q = q_0 k_w$) was considered equal to 3.9 for regular frame buildings and 3.6 for the regular plane frame-wall building.

Reinforcement schemes for DDBD and FBD procedures have been defined and the criterion for ductile behaviour of concrete sections defined in the Eurocode 8 [40] fulfilled (Ductility Class Medium – DCM). Minimum and maximum longitudinal reinforcement adopted for beams are defined in Eurocode 2 (2010), Section 9.2.1.1. ($A_{s,min} = 0.26 f_{ctm} / f_{yk} b_t d^{(1)}$ with a minimum value of $0.0013 b_t d$). The maximum value for beam reinforcement area is $0.04 A_c^{(2)}$.

For columns, minimum and maximum longitudinal reinforcement as defined in Eurocode 2 Part 1 (2010), Section 9.5.2. ($A_{s,min} = 0.10 N_{ED} / f_{yd}^{(3)}$ or $0.002 A_c$) was taken in consideration. The maximum value for column reinforcement area is $0.04 A_c$.

For walls, minimum and maximum longitudinal reinforcement as defined in Eurocode 2 Part 1 (2010), Section 9.6.2. ($0.002 A_c \leq A_{sv} \leq 0.04 A_c^{(4)}$).

Table VI and Table VII provide the average reinforcement ratio obtained for configurations 1, 2 and 3 designed with the DDBD and FBD methodology, respectively.

It can be stated from the Table VI for frame structures 1 and 2 designed with DDBD procedure the amount of total average reinforcement is 39.5% and 5.1% higher when compared with FBD procedure, respectively. In total, the amount of total longitudinal reinforcement is about 40% higher for the regular frame structure (configuration 1) designed with DDBD methodology and this is due to the increase of the reinforcement in both structural elements (beams and columns, but significantly more in columns). Thus, it can be realized that structures designed according to DDBD procedure

⁽¹⁾ $A_{s,min}$ – minimum longitudinal reinforcement; f_{ctm} – mean value of axial tensile strength of concrete; f_{yk} – characteristic yield strength of reinforcement; b_t – mean width of the tension zone; d – Effective depth of a cross-section; ⁽²⁾ A_c – total cross-sectional area of a concrete section; ⁽³⁾ $A_{s,min}$ – minimum longitudinal reinforcement; N_{ED} – design value of the applied axial force (tension or compression); f_{yd} – design yield strength of reinforcement; ⁽⁴⁾ A_{sv} – area of vertical reinforcement.

Table IV Design parameters for frame structures under study (DDBD procedure)

Conf., i	H_n [m]	h_1 [m]	$h_i (i > 1)$ [m]	Δ_{dtop} [m]	H_e [m]	m_e [ton]	Δ_y [m]	Δ_d [m]	μ	ξ_{eq} [%]	T_e [s]	V_{base} [kN]
1	24	3	3	0.465	16.62	365.71	0.229	0.345	1.51	10.52	2.26	905.40
2	26	5		0.512	18.70	387.10	0.249	0.384	1.54	10.27	2.49	799.62

Table V Design parameters for different base shear sharing between wall and frame in the dual structure (DDBD procedure)

β_F	θ_{CF}	H_e [m]	m_e [ton]	Δ_d [m]	μ_F	μ_w	ξ_F [%]	ξ_w [%]	T_e [s]	V_{base} [kN]
0.40	0.032	17.10	412.60	0.304	1.29	3.08	0.091	0.150	2.05	1154.00
0.50	0.028	18.4	446.70	0.344	1.36	3.67	0.097	0.153	2.31	981.00
0.60	0.020	16.8	429.30	0.329	1.43	6.73	0.100	0.1700	2.21	1032.00

Table VI Average reinforcement ratio in %

ρ (%)	Frame	DDBD	FBD	Difference (%)
Average – Frame	1	2.12	1.52	39.5%
	2	2.05	1.95	5.1%
Outer columns – average	1	2.85	2.00	42.5%
	2	2.31	2.33	-0.9%
Inner columns – average	1	2.14	1.41	51.8%
	2	2.09	2.22	-5.9%
Columns average	1	2.41	1.64	47.0%
	2	2.19	2.22	-1.4%
Beam outer bay	1	1.83	1.41	29.8%
	2	1.89	1.61	1.2%
Beam inner bay	1	1.84	1.42	29.6%
	2	1.90	1.61	1.2%

Table VII Average reinforcement ratio in % – β_F

ρ (%)	β_F	DDBD	FBD	Difference (%)
TOTAL	0.4	1.31	1.32	- 0.5%
	0.5	1.29	1.32	- 2.3%
	0.6	1.24	1.32	- 6.2%
Frame	0.4	1.93	1.95	- 1.2%
	0.5	1.91	1.95	- 2.5%
	0.6	1.95	1.95	0.0%
Wall	0.4	0.70	0.68	1.5%
	0.5	0.67	0.68	- 2.0%
	0.6	0.57	0.68	- 16.5%
Outer columns average	0.4	2.36	2.85	- 17.1%
	0.5	2.46	2.85	- 13.6%
	0.6	2.46	2.85	- 13.6%
Inner columns average	0.4	2.55	2.13	19.8%
	0.5	2.49	2.13	16.8%
	0.6	2.49	2.13	16.8%
Columns average	0.4	2.31	1.67	38.3%
	0.5	2.42	1.67	44.9%
	0.6	2.74	1.67	64.1%
Beam outer bay	0.4	1.40	1.50	- 7.0%
	0.5	1.35	1.50	- 10.4%
	0.6	1.35	1.50	- 10.4%
Beam inner bay	0.4	1.40	1.54	- 9.6%
	0.5	1.35	1.54	- 12.9%
	0.6	1.35	1.54	- 12.9%

led, as expected, to the development of the desired mechanism. In fact, this procedure shows to be very rational and effective in structural design as it controls structural displacements and thus it controls damage level (assuring a uniform distribution of damage in height) and collapse risk.

Revising Table VII it can be stated that DDBD procedure led to a structure with higher amounts of average of reinforcement ratio for regular dual systems. The most noteworthy value is observed for the fraction of base shear supported by the frame (β_f) of 0.40, ranging about 15%. This tendency is inverted for the irregular in elevation dual systems, where the values of average reinforcement ratios are similar or lower than those obtained by means of FBD procedure for different values of the total fraction of base shear supported by the frame (β_f) of 0.40, 0.50 and 0.60, respectively.

4.4 Performance assessment

The set of frames designed according to DDBD and FBD procedures have been seismically assessed through nonlinear static (Pushover) analyses and nonlinear dynamic time-history analyses. For nonlinear static analyses, the N2 method was performed according to the Eurocode 8 [40] part 1 Section 4.3.3.4.2.2, using two vertical distributions of the lateral loads, uniform and modal patterns.

In the framework of performance-based design, several performance limit states are selected and identified, in terms of strain and drift limits (see [33]).

The results of Pushover analysis and Nonlinear Time-History analyses carried out on configurations 1, 2 and 3, designed according to DDBD and FBD procedures, are shown hereunder. In Figure 17, the capacity curves obtained considering a first mode proportional load pattern for both design procedures are depicted, representing in these curves the target displacement obtained by N2 method (EC8) and corresponding base shear (marked with a red cross). The results obtained with N2 method for the frame-wall structure designed by both procedures are also presented for different seismic intensities (i.e. for return periods of 475, 1344 and 2475 years).

For Configuration 1 designed according to DDBD procedure a base shear 29% higher when compared with the base shear obtained for the frame structure designed with FBD procedure is reached. For Configuration 2 and for both design procedures the capacity curves are similar, however the frame structure designed with FBD exhibits less strength degradation.

From Figure 17 c) to f) it is clear that only the frame-wall designed with DDBD with a β_f very similar to the one designed with FBD (Figure 17 e) has a different capacity, being less stiff and with lower strength than all the other frame-walls.

Figures 17 a) and 17 b) also present the results obtained by means of the N2 method and median results from nonlinear time history analyses for the structure designed with DDBD procedure, namely the maximum top displacement (and the correspondent base shear) and the maximum base shear (with the correspondent top displacement) for different seismic intensities (i.e. for return periods of 72, 475 and 2475 years). From the presented results, one can observe that the N2 method leads to conservative maximum roof displacements when compared with the nonlinear dynamic analysis

results (THA – seismic intensity correspondent to 475 years return period).

Figures 18 and 19 show the deformed shape of studied frames, for both design procedures, when the ultimate strain of steel is reached. In these figures, green marks correspond the first yield of steel, yellow marks the first fracture of steel, red marks the first crushing of core concrete, and orange marks the first spalling of concrete cover.

Figures 18 and 19 show that the seismic assessment of the final frame structure designed with DDBD procedure leads to the development of an inelastic mechanism corresponding to the expected one (i.e. plastic hinges formation at beam-ends and base of the columns). For the configurations designed according FBD procedure, when the ultimate strain of steel is reached in some fibres, some crushing of concrete occurs at some columns ends located at the third floor (Figure 18 a). This undesirable behaviour is not verified for the frame designed with DDBD method.

The inter-story drift ratio are presented in Figure 20 for both design procedures and nonlinear analyses performed, considering the seismic action correspondent to the return period of 475 years. In these figures, THA stands for nonlinear time history analyses and N2 for the method used in the nonlinear static analyses. For the THA results, it is shown that the outcomes corresponding to the mean and the mean \pm standard deviation.

From Figure 20 a) and b), it can be observed that the design drift limit imposed for the first floor by the DDBD ($\theta_c = 2.5\%$) in terms of inter-storey drift ratio is never reached, whatever configuration and design method is considered. The Overall behaviour of the frames is consistent with the design assumptions according to the DDBD procedure. The results regarding the inter-story drift at lower stories show a different trend from the expected one for a frame building, i.e. the inter-story drift is not decreasing along the height of the building. This can be explained by the modelling assumptions where fixed bases have been considered for the columns. It can be remarked that the target performance level considered in the DDBD design procedure is not reached. Furthermore, for frame structures (Configurations 1 and 2) designed according to the FBD procedure present smaller displacements and interstorey-drift ratios in the lower stories when compared with those obtained for same case study designed by means of DDBD procedure; i.e. the results are more conservative for lower stories. The opposite occurs at the middle stories (see Figure 20 a) and b)) where, for the FBD procedure, the interstorey-drift ratio reaches 2.5%.

Once more, from the presented results presented in Figure 20 a) and b) one can observe that the N2 method generally leads to conservative displacements and inter-story drift when compared with the nonlinear dynamic analysis.

Revising the results presented in Figure 20 c), it is clear that the design deformation profile defined with the nonlinear static analyses has been correctly matched (i.e. it is very similar to the one obtained with THA). Furthermore, when one compares the average of the maximum recorded displacements and inter-story drifts with the design values for the performance level considered, these are much smaller, far from being reached for the above mentioned seismic intensity.

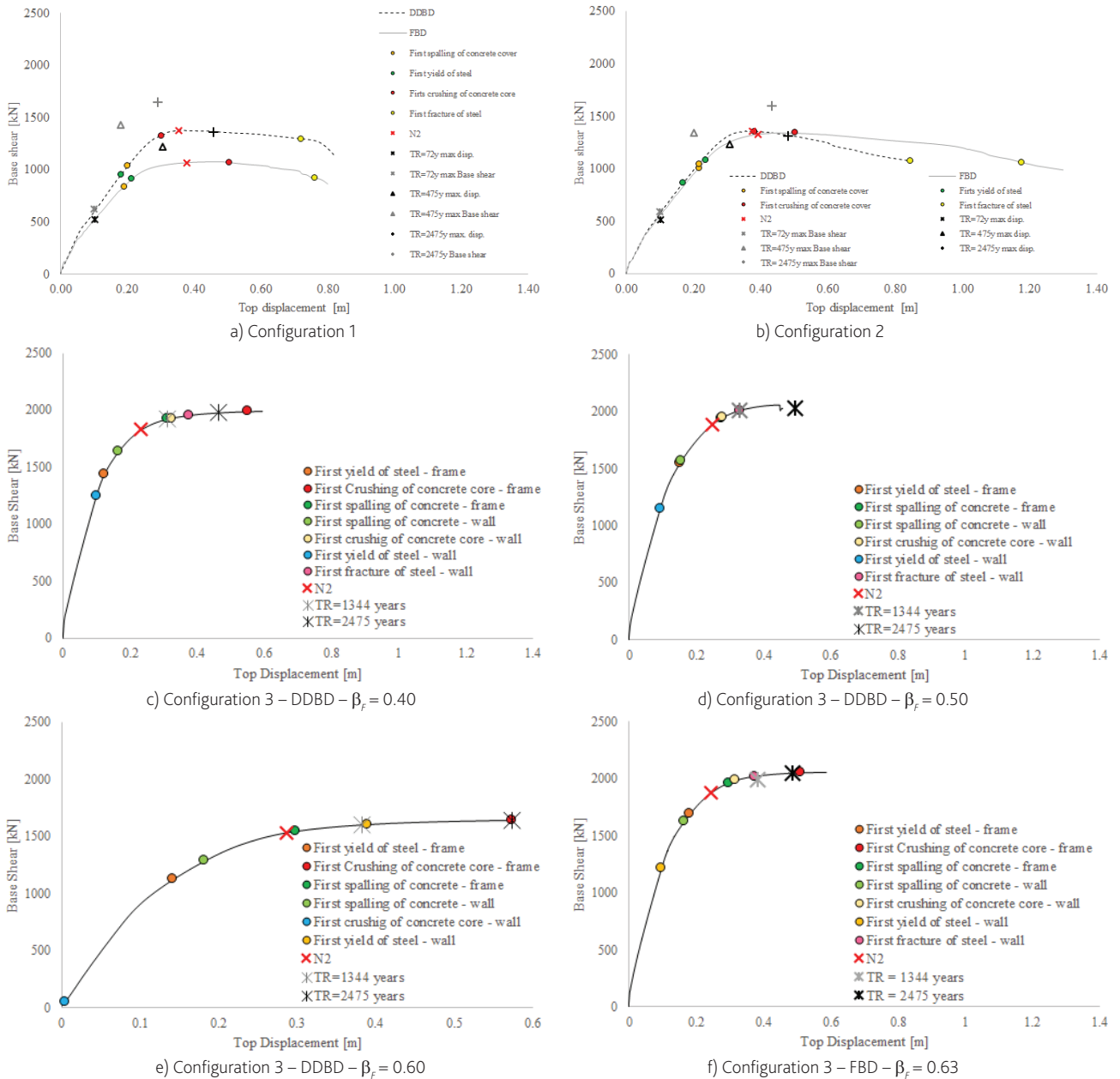


Figure 17 Capacity curves

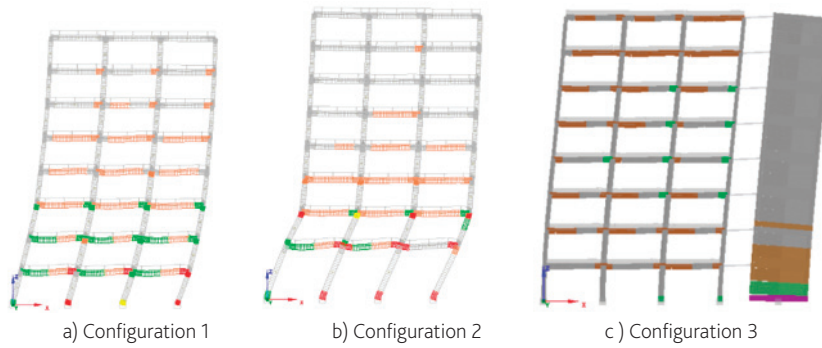


Figure 18 Deformed shape for DDBD procedure – Reached ultimate strain of steel

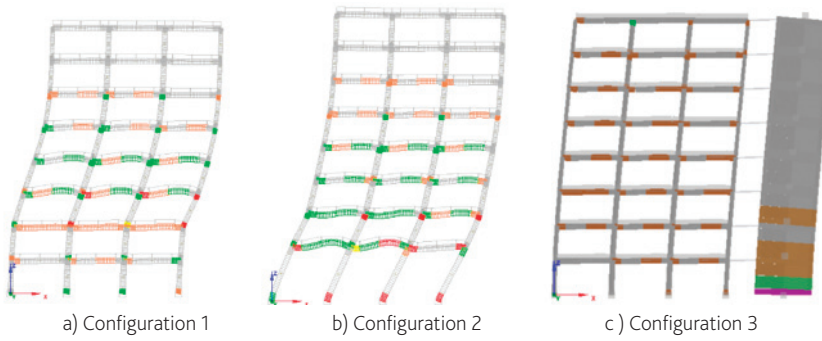


Figure 19 Deformed shape for FBD procedure – Reached ultimate strain of steel

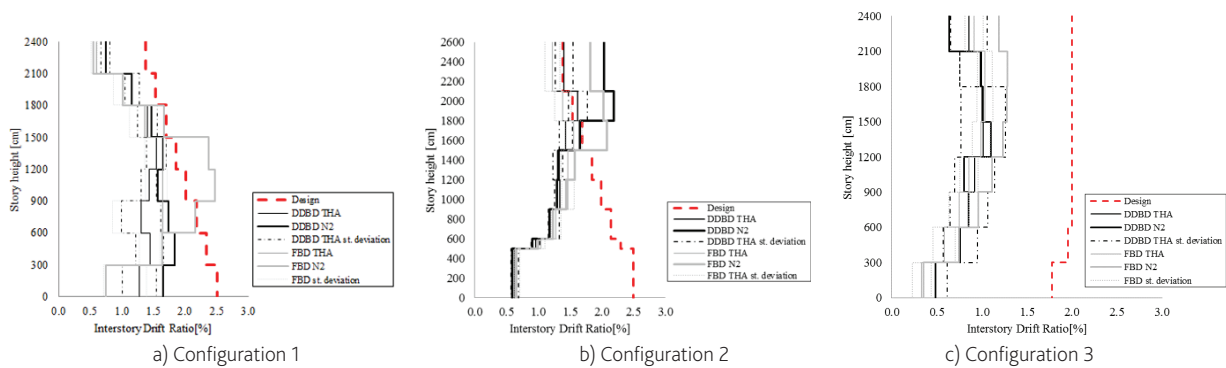


Figure 20 Inter-story drift profile

The dual systems designed with DDBD methodology result in structures with higher amounts of longitudinal reinforcement for frames, but this trend is inverted in walls. Nevertheless, the DDBD methodology allows an enhanced spread of nonlinear behaviour throughout the frame structure, leading to the development of a mechanism corresponding to the expected one (i.e. plastic hinges formation at beam-ends and base of the wall). The outcome of the DDBD applied to dual system is that the design procedure allows to the designer to directly control the forces developed in the structure by choosing strength proportions at the start of the design procedure [33].

Finally, with the results obtained, and essentially for the frame-wall structure, it is clear that the design drift limit imposed according to the DDBD methodology, in terms of inter-storey drift ratio, is never reached. One reason for this is certainly related to the definition of the displacement response spectrum. This displacement spectrum for damping values higher than the nominal value of 5% of critical, will be obtained by applying scaling factors to the 5% damped ordinates. These scaling factors, proposed by design codes, are independent of the nature of the expected ground shaking. In fact, some studies have shown (e.g. [47]) that the scaling factors for different damping levels vary with magnitude and distance, putting in evidence a dependence of the scaling on the duration of shaking that increases with the damping ratio. The work of Bommer and Mendis [48] has shown that the spectral scaling factors vary with seismological features: magnitude, distance, duration and to the site conditions. These findings should be considered in future work to the proper definition displacement response spectra for design.

5 Conclusions

The objective of this paper was to investigate and clarify some aspects of an emergent design method, the DDBD method, which is gaining popularity in both the research and practicing earthquake engineering communities. This method is fast and simple to apply, allowing to design a structure to satisfy a pre-defined drift level. All the steps of the DDBD method, in particular for RC frame and dual frame-wall structures, are investigated.

A review and background assessment of performance-based seismic design procedures has been carried out, especially displacement-based procedures, based on which the design procedure known as DDBD is selected. The equivalent viscous damping which has been identified as a crucial parameter of the DDBD methodology was investigated. A comprehensive inventory of the expressions available in the literature to correlate the effective period, the design ductility and the equivalent damping is carried out and a systematic comparison of the numerous existing expressions for the equivalent damping is performed. A comparison is also performed between the equivalent damping obtained from numerical NLTHA for different types of ground motion and the equivalent damping obtained with two recent theoretical formulations proposed respectively by Blandon-Priestley and Dwairi-Kowalsky and the results discussed in detail. The main outcome of this comparison is that, except in some specific conditions that require additional investigation (i.e. very small effective periods, effective periods greater than the corner period of the displacement response spectrum and some

cases of low ductility), the different approaches lead to a rather important scattering of the results, with a range of variation of the error between the damping values obtained from numerical and theoretical approaches around 25%. Furthermore, it appears impossible to determine which approach is better, as the difference in terms of accuracy related to the assumed shape of the design spectrum is greater than the difference related to the choice of one or another viscous damping formulation. Therefore, it is thought that the choice between both formulations can be based on simplicity, which gives a clear advantage to the Dwairi-Kowalsky proposal but also provides argument for the current choice of an even simpler formulation made in pre-normative documents.

A set of RC plane structures (two frames, regular and irregular in height, and a frame-wall structures, designed for different strength proportions carried by the frame) are characterized and designed according to the DDBD and to the traditional force-based design method as proposed in European standard for seismic design, the Eurocode 8, and their performance is evaluated. It is found that the global behaviour of the case study plane frame structures with the DDBD is consistent with the design assumptions according to this design procedure. For the earthquake intensity considered in the design it is observed that the target performance level is not reached, whatever the design method considered. No special improvements are noticed for DDBD in comparison with FBD but it is worth to note that for this seismic intensity the frames are performing adequately. The set of buildings designed with the DDBD methodology resulted in structures with slightly higher amounts of longitudinal reinforcement in the columns. However, based on the results obtained for the set of frame buildings analysed, it seems that, in general, the DDBD methodology leads to the development of a mechanism corresponding to the expected one. One can point out that the DDBD method has been successfully verified for a set of structural typologies, regular and irregular, leading, in most of the cases studied, to a better seismic design than the traditional procedures.

The advantage of the DDBD applied to plane structures is that the design procedure allows the designer to have direct control over the forces developed in the structure by choosing strength proportions at the start of the design procedure.

Moreover, from the results obtained, and mainly for the dual frame-wall structure, one can conclude that the design drift limit imposed in accordance to the DDBD methodology in terms of inter-storey drift ratio is never reached. One reason for this is certainly related to the definition of the displacement response spectrum, used for the DDBD procedure and defined in the Eurocode 8. This displacement spectrum, as it is also proposed in other design codes, for critical damping values higher than the nominal value of 5%, will generally be obtained by applying scaling factors to the 5% damped ordinates. These scaling factors, proposed by design codes, are functions of the damping ratio and, in some cases, the response period, but are independent of the nature of the expected ground shaking. Future work is needed to determine appropriate spectral scaling factors, which would consider different seismological features. This would be essential for the adequate definition of displacement response spectra for design, thus leading to more improved estimates of the design motions.

References

- [1] Park R.; Paulay, T. (1975) – *Reinforced Concrete Structures*, John Wiley & Sons. New York, 769p.
- [2] Priestley, M.J. (1993) – "Myths and fallacies in earthquake engineering-conflicts between design and reality", *Bulletin of the New Zealand National Society for Earthquake Engineering*, Vol. 26(3), 329–341.
- [3] Priestley, M.N.J.; Grant, D. N.; Blandon, C.A. (2005) – "Direct Displacement-based Seismic Design", NZSEE Conference.
- [4] Fib. (2003) – "Displacement-based Seismic Design of Reinforced Concrete Buildings. State-of-the-art Report". Bulletin 25, Federation International de Beton, Lausanne Switzerland, 196.
- [5] Sullivan, T.J.; Calvi, G.M.; Priestley, M.J.N.; Kowalsky, M.J. (2003) – "The Limitations and Performances of Different Displacement-Based Design Methods". *Journal of Earthquake Engineering*, Vol. 7 (SP1), 201-241.
- [6] Priestley M.J.; Kowalsky M.J. (2000) – "Direct Displacement-Based Seismic Design of Concrete Buildings". *Bulletin of the New Zealand National Society for Earthquake Engineering*, Vol. 44(2), 145–165.
- [7] Shibata, A.; Sozen, M.A. (1976) – "Substitute-Structure Method for Seismic Design in R/C." *Journal of Structural Division*, ASCE, Vol. 102, (12), 3548-3566.
- [8] Gulkan, P.; Sozen, M.A. (1974) – "Inelastic Responses of Reinforced Concrete Structures to Earthquake Motion". *ACI Journal*, ACI, Vol. 17(12), 604-610.
- [9] Sozen, M.A. (1981) – *Review of Earthquake Response of RC Buildings with a View of Drift Control State-of-art in Earthquake Engineering*.
- [10] Moehle, J.P. (1984) – "Strong Motion Drifts Estimates for R/C Structures". *Journal of Earthquake Engineering*, ASCE, Vol. 110 (9), 1988-2001.
- [11] Saiidi, M.; Sozen, M. A. (1979) – "Simple and Complex Models for Nonlinear Seismic Response of Reinforced Concrete Structures". SRS No. 465, Univ. of Illinois, Urbana.
- [12] Qi, X.; Moehle, J.P. (1991) – "Displacement Design Approach for Reinforced Concrete Structures Subjected to Earthquakes", Report NO UCB/EERC-91/02, EERC, UC Berkeley, CA, 186 pp.
- [13] Shimazaki, K.; Sozen, M. A. (1984) – "Seismic drift of reinforced concrete structures," *Tech. Res. Rep. of Hazama-Gumi*, Tokyo, 145-166.
- [14] Moehle, J.P. (1992) – "Displacement-Based Design of RC Structures Subjected to Earthquakes. Earthquake Spectra", *EERI*, Vol. 8 (3), 403-428.
- [15] Kowalsky, M.J.; Priestley, M.J.N.; MacRae, G.A. (1994) – "Displacement-Based Design: A Methodology for Seismic Design Applied to Single Degree of Freedom Reinforced Concrete Structures. Structural Systems", Research Report, University of California, San Diego.
- [16] Kowalsky, M.J.; Priestley, M.J.N.; MacRae, G.A. (1995) – "Displacement-Based Design of RC Bridge Columns in Seismic Regions". *Earthquake Engineering and Structural Dynamics*, Vol. 24(12), 1623-1643.
- [17] Calvi, G.M.; Kingsley, G.R. (1995) – "Displacement-Based Seismic Design of Multi- Degree-of Freedom Bridge Structures", *Earthquake Engineering and Structural Dynamics*, Vol. 24, 1247-1266.
- [18] Priestley, M.J.N.; Calvi, G.M. (1997) – "Concepts and Procedures for Direct Displacement-Based Design and Assessment". *Proc., Seismic Design Methodologies for the Next Generation of Codes*, Fajfar, P. and Krawinkler, H. (Eds.), Bled, Slovenia, June 24-27, 1997, A.A. Balkema, Rotterdam, 171-182.
- [19] Kowalsky, M.J. (2002) – "A Displacement-Based Approach for the Seismic Design of Continuous Bridges". *Earthquake Engineering and Structural Dynamics*, Vol. 31 (3), 719-747.
- [20] Priestley, M.J.N.; Calvi, G.M. (2003) – "Direct Displacement-Based Seismic Design of Concrete Bridges". *Proc.: ACI 2003 International Conference: Seismic Bridge Design and Retrofit for Earthquake Resistance*, December 8-9, 2003, La Jolla, CA.
- [21] Calvi, G.M.; Pavese, A. (1995) – "Displacement-Based Design of Building Structures. European Seismic Design Practice: Research and Application", *Proceedings of the Fifth SECED Conference*. United Kingdom, Oct. 26-27.
- [22] Priestley, M.J.N.; Kowalsky, M.J.; Ranzo, G.; Benzoni, G. (1996) – "Preliminary Development of Direct Displacement-Based Design for Multi-Degree of Freedom Systems", *Proc.: 65th Annual SEAOC Convention*, Maui, Hawaii, U.S.A., 47-66.
- [23] Priestley, M.J.N.; Calvi, G.M. (1997) – "Concepts and Procedures for Direct Displacement-Based Design and Assessment". *Proc., Seismic Design Methodologies for the Next Generation of Codes*, Fajfar, P. and Krawinkler, H. (Eds.), Bled, Slovenia, June 24-27, 1997, A.A. Balkema, Rotterdam, 171-182.
- [24] Priestley, M.J.N. (1998a) – "Brief Comments on Elastic Flexibility of Reinforced Concrete Frames and Significance to Seismic Design". *Bulletin of the New Zealand Society for Earthquake Engineering*, Vol.31 (4), 246-259.
- [25] Priestley, M.J.N. (1998b) – "Direct Displacement-Based Seismic Design of Buildings". *Proc., Asia-Pacific Workshop on Seismic Design and Retrofit of Structures*, Taipei, China, August 10-12, NCREC, 549-569.
- [26] Loeding, S.; Kowalsky, M.J.; Priestley, M.J.N. (1998) – "Displacement-Based Design Methodology Applied to R.C. Building Frames". Structural Systems Research Report, SSRP -98/06, University of California, San Diego.
- [27] Priestley, M.J.; Kowalsky, M.J. (2000) – "Direct Displacement-Based Seismic Design of Concrete Buildings". *Bulletin of the New Zealand National Society for Earthquake Engineering*, Vol. 44(2), 145–165.
- [28] Kowalsky, M.J.; Ayers, J.P. (2001) – "Investigation of Equivalent Viscous Damping for Direct Displacement-Based Design". *Proc.: The Third U.S.-Japan Workshop on Performance-Based Design*.
- [29] Priestley, M.J.N. (2003) – "Myths and Fallacies in Earthquake Engineering, Revisited". The 9th Mallet Milne Lecture, IUSS Press (Rose School), Pavia, Italy, 121 pp.
- [30] Priestley, M.J.; Calvi G.M.; Kowalsky M.J. (2007) – "Displacement-Based Seismic Design of Structures". IUSS Press, Pavia, Italy.
- [31] Pettinga, J.D.; Priestley, M.J.N. (2005) – "Dynamic behaviour of reinforced concrete frames designed with direct displacement-based design". *Journal of Earthquake Engineering*. Vol 9 (2), 309-330.
- [32] Sullivan, T.; Priestley M.J.; Calvi G.M. (2006) – "Seismic Design of Frame-Wall Structures". ROSE Research Report No.2006/02, IUSS Press, Pavia.

- [33] Massena, B. (2017) – *Reliability Assessment of the Direct Displacement-Based Design Methodology*, PhD thesis, Instituto Superior Técnico, Universidade de Lisboa
- [34] Calvi, G.M.; Sullivan, T.J. editors (2009) – *A Model Code for the Displacement-Based Seismic Design of Structures*, DBD09, IUSS press, Pavia, Italy.
- [35] Sullivan, T.J.; Calvi, G.M.; Priestley, M.J.N. editors (2012) – *A Model Code for the Displacement-Based Seismic Design of Structures*, DBD12, IUSS press, Pavia, Italy.
- [36] Powell, G. (2008) – *Book review: Displacement-Based Seismic Design of Structures, Earthquake Spectra*, Volume 24, No. 2, pages 555–557
- [37] Sullivan, T.J.; Bono, F.; Magni, F.; Pinho, R.; Calvi, G.M. (2012) – "DBDsoftware: A program for the displacement-based seismic design of structures, Beta Version". EUCENTRE, www.eucentre.it.
- [38] Sullivan, T.; Bono, F.; Nievas, C.I.; Magni, F.; Calvi, G.M. (2014) – "DBDsoft: A program for the displacement-based seismic design of structures, Beta Version" EUCENTRE, www.eucentre.it.
- [39] Sullivan, T. (2014) – "Analysis methods for Performance Base Design in future version of EN1998", *2nd European conference in Earthquake Engineering and Seismology*, Aug. 25-29, Istanbul, Turkey.
- [40] EN 1998-1:2004. Eurocode 8 – *Design of Structures for Earthquake Resistance – Part 1: General Rules. Seismic Actions and Rules for Buildings*. CEN. Brussels. Belgium.
- [41] Beyer, K. (2014) – "Future Directions for Reinforced Concrete Buildings in Eurocode 8", *2nd European conference in Earthquake Engineering and Seismology*, Aug. 25-29, Istanbul, Turkey.
- [42] Calvi, G.M.; Kingsley, G.R. (1995) – "Displacement-Based Seismic Design of Multi-Degree of Freedom Bridge Structures", *Earthquake Engineering and Structural Dynamics*, Vol. 24, 1247-1266.
- [43] Dwairi, H.M.; Kowalsky, M.J. (2004) – "Investigation of Jacobsen's Equivalent Viscous Damping Approach as applied to Displacement-Based Seismic Design", *13th World Conference on Earthquake Engineering*, Aug. 1-6, Vancouver, Canada. Paper No 228.
- [44] Blandon, C.A.; Priestley, M.J.N. (2005) – "Equivalent viscous damping equations for direct displacement design". *Journal of Earthquake Engineering*, Vol. 9 (special issue 2), 257-27
- [45] SeismoSoft (2016) – "SeismoStruct – A Computer Program for Static and Dynamic Nonlinear Analysis of Framed Structures", Available from URL: www.seismosoft.com
- [46] FineLg, (2003) – User's manual, V9.2, Greisch Info – Department ArGEnCo ULg
- [47] Blandon, C.A. (2004) – *Equivalent Viscous Damping Equations for Direct Displacement-Based Design*, MSc thesis, Rose School, Università degli Studi di Pavia.
- [48] Bommer, J.; Mendis, R. (2005) – "Scaling of spectral displacement ordinates with damping ratio". *Earthquake Eng Struct. Dyn.*, N° 34, 145-165
- [49] Denoel, V. (2001) – "Generation of Spectrum Compatible Accelerograms", Research Report, Université de Liège, Belgique.
- [50] Grant, D, N.; Blandon C.A.; Priestley M.J.N (2005) – "Modelling Inelastic Response in Direct Displacement-Based Design". ROSE Research Report No.2005/03, IUSS Press, Pavia.
- [51] NP EN 1998-1:2007 – Portuguese National Annex.